How to cite: *Angew. Chem. Int. Ed.* **2021**, *60*, 14022–14029
International Edition: doi.org/10.1002/anie.202102227
German Edition: doi.org/10.1002/ange.202102227

Supramolecular Chemistry

Tuneable Control of Organocatalytic Activity through Host–Guest Chemistry

*Guotai Li[+], Fanny Trausel[+], Michelle P. van der Helm, Benjamin Klemm, Tobias G. Brevé, Susan A. P. van Rossum, Muhamad Hartono, Harm H. P. J. Gerlings, Matija Lovrak, Jan H. van Esch, and Rienk Eelkema**

Abstract: *Dynamic regulation of chemical reactivity is important in many complex chemical reaction networks, such as cascade reactions and signal transduction processes. Signal responsive catalysts could play a crucial role in regulating these reaction pathways. Recently, supramolecular encapsulation was reported to regulate the activities of artificial catalysts. We present a host-guest chemistry strategy to modulate the activity of commercially available synthetic organocatalysts. The molecular container cucurbit[7]uril was successfully applied to change the activity of four different organocatalysts and one initiator, enabling up- or down-regulation of the reaction rates of four different classes of chemical reactions. In most cases CB[7] encapsulation results in catalyst inhibition, however in one case catalyst activation by binding to CB[7] was observed. The mechanism behind this unexpected behavior was explored by NMR binding studies and pKa measurements. The catalytic activity can be instantaneously switched during operation, by addition of either supramolecular host or competitive binding molecules, and the reaction rate can be predicted with a kinetic model. Overall, this signal responsive system proves a promising tool to control catalytic activity.*

Introduction

Dynamic regulation of chemical reactivity is important in many complex chemical reaction networks such as cascade reactions and signal transduction processes.[1,2] In nature, these processes are heavily regulated by enzymatic catalysis, where the activity of these catalysts themselves are modulated to render such reaction networks responsive to external signals, changes in substrate levels or changes in the environment.[3] Responsive artificial catalysts could play similar roles in chemical reaction networks, where regulation of catalytic activity is crucial to achieve efficient temporal and spatial control over chemical transformations without unnecessary waste or off-cycle reaction pathways. Furthermore, the reversible de-activation/re-activation of catalysts by external signals can make such artificial systems highly responsive to environmental stimuli, analogous to signal-responsive enzyme catalysis in nature.[2,4] Still, to this date such responsive catalysts remain very rare, have a narrow application scope or rely on extensive synthetic efforts.[5] Recently, there have been reports of regulation of the activity of synthetic catalysts[6] by supramolecular encapsulation including rotaxanes,[7–9] resorcin[4]arene,[10–12] cyclodextrin[13] and cucurbit[7]uril[14–18] which is of high interest because it enables precise, reversible and responsive control over reaction rates by adjusting the amount of available catalyst in situ. Among them, cucurbit[7]uril (CB[7]) is a widely applied molecular container, a cyclic glycoluril heptamer that binds strongly to small neutral and cationic compounds.[19–21] CB[7] is commercially available, non-toxic and relatively soluble in water, which makes it possible to be used in aqueous environments or even biological systems. Examples of CB[7] catalytic activity regulation include the regulation of transition metal catalysts embedded in gold nanoparticles in cells,[14] the enhancement of photocatalytic H_2 evolution,[15] promotion of the Fenton oxidation through supramolecularly modulated ferrocene catalysts,[16] and control over copper catalyzed alkyne azide click chemistry.[17] Most of these examples focus on transition metal catalysis. To date, only Leigh and coworkers reported a switchable secondary amine catalyst based on a rotaxane,[7–9] but that system has a highly specialized design to enable complex formation between host and catalyst. As of now no generic method is available for tuneable catalytic activity regulation of common simple, commercially available organocatalysts. Since organocatalysis is emerging as one of the main branches of synthetic science,[22] we hypothesize that the exploration of CB to control readily accessible and widely used organocatalysts, would highly broaden the application scope of this method.

Herein we report a strategy to change and tune the catalytic activity in situ of diverse, widely applied organocatalysts by host-guest encapsulation in aqueous environment. Specifically, with supramolecular encapsulation we can control the catalytic activity of four different organocatalysts in various bond forming reactions: primary amine (**C1**: aniline

[*] G. Li,[+] Dr. F. Trausel,[+] Dr. M. P. van der Helm, B. Klemm, T. G. Brevé, Dr. S. A. P. van Rossum, M. Hartono, H. H. P. J. Gerlings, Dr. M. Lovrak, Prof. Dr. J. H. van Esch, Dr. R. Eelkema
Department of Chemical Engineering
Delft University of Technology
van der Maasweg 9, 2629 HZ Delft (The Netherlands)
E-mail: r.eelkema@tudelft.nl

[+] These authors contributed equally.

Supporting information and the ORCID identification number(s) for the author(s) of this article can be found under: https://doi.org/10.1002/anie.202102227.

and **C5**: benzimidazole-amine) catalyzed hydrazone formation, tertiary amine (**C2**: DABCO) catalyzed allylic substitution, secondary amine (**C3**: prolinol) catalyzed aldol formation, as well as the oligomerization of maleimide initiated by an amine initiator (**C4**: nornicotine) (Scheme 1c). These reactions all proceed in aqueous media under biologically relevant conditions.[23] In most of the cases, reaction rates can be down- and upregulated by binding the catalyst to CB[7] and subsequently releasing it by adding a competitive strong binder for CB as a chemical signal.

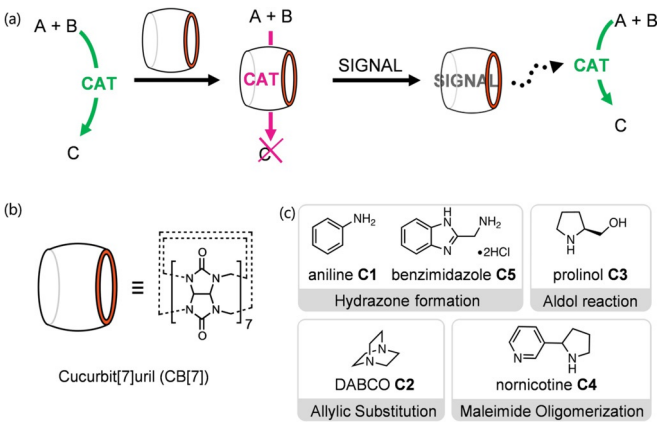

Scheme 1. The concept of using host-guest chemistry to control the activity of organocatalysts. a) Schematic representation of CB[7] binding to the organocatalyst (CAT), hindering its catalytic activity. Addition of the stronger binding signal leads to the release of the catalyst and restores its catalytic activity; b) Structure of CB[7]; c) Organocatalysts **C1**–**C5** and their associated reactions.

Results and Discussion

System design considerations and selection of organocatalysts

The applied catalysts (Scheme 1c) were first selected based on the binding affinity with CB[7]. CB[7] binds strongly to somewhat hydrophobic, positively charged molecules with an appropriate size for the CB[7] cavity.[12] To be able to use CB[7] to modify catalyst activity by encapsulation, it is essential that the catalyzed reaction works in aqueous environments, and that the affinity of the catalysts with CB[7] is high enough to ensure that the majority of catalyst is encapsulated at the operational concentrations. Meanwhile, the substrates and products should not bind to CB[7]. On the other hand, the signal molecules should have a much larger affinity for CB[7] than the catalyst, to allow efficient liberation of the catalyst through competitive binding, analogous to the indicator displacement assay (IDA).[24] From this principle, four organocatalysts and one organic initiator: aniline **C1**, DABCO **C2**, L-prolinol **C3**, nornicotine **C4** (an initiator for maleimide oligomerization), 1*H*-benzimidazole-2-methanamine **C5**, and three signal molecules (**SG1**–**3**) were selected and used separately in a range of reactions. NMR binding studies of these catalysts and initiator also indicated their affinity to CB[7] (Figures S5–S10). Table 1 summarizes the binding constants of CB[7] with **C1**–**5** and **SG1**–**3**.

Table 1: Binding constants of organocatalysts and signal molecules with CB[7].

Compound	Structure	K_a [M^{-1}]
C1	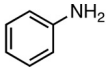	$(1.3 \pm 0.038) \times 10^5$ [a]
C2		$(3.6 \pm 0.032) \times 10^5$ [b]
C3	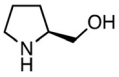	$(5.75 \pm 0.16) \times 10^3$ [b]
C4	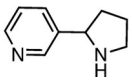	$(4.6 \pm 0.035) \times 10^4$ [b]
C5	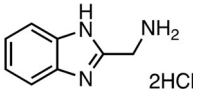	$(2.8 \pm 0.20) \times 10^5$ [a]
SG1	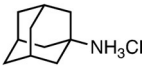	$(4.2 \pm 1.0) \times 10^{12}$ [c]
SG2	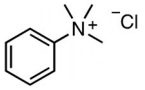	$(2.5 \pm 0.6) \times 10^8$ [d]
SG3	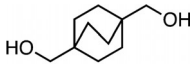	$(6.1 \pm 0.5) \times 10^9$ [e]

[a] Measured by ITC in 10 mM sodium phosphate buffer pH 6.0, 25 °C; [b] Measured by ITC in 100 mM sodium phosphate buffer pH 7.4, 25 °C; [c] Values from Ref. [19], measured by NMR in NaO_2CCD_3 (50 mM) buffer, pH 4.74; [d] Values from Ref. [25], measured by NMR in D_2O, 25 °C; [e] Values from Ref. [26], measured by ITC in H_2O, 25 °C.

Generally, the binding constants of the catalysts are in the range of $\approx 10^3$–$10^5\ M^{-1}$ and the signal molecules are $\approx 10^8$–$10^{12}\ M^{-1}$, while the reaction substrates and products are chosen such that they bind with $K_a < 10\ M^{-1}$ (Supporting information Table S5).

Control over aniline (C1) catalysis in hydrazone formation

We first focused on the hydrazone formation reaction, a widely applied condensation reaction between an aldehyde and a hydrazide that takes place in aqueous buffer and is accelerated by a variety of organocatalysts.[27,28] Aniline **C1** is often used as a catalyst in this reaction, although in (super)-stoichiometric amounts because of its low efficiency.[29,30] The reaction between aldehyde **SM1** (0.4 mM) and hydrazide **SM2** (0.04 mM) in aqueous buffer (10 mM sodium phosphate buffer pH 6.0) leads to the formation of hydrazone product **P1** (Figure 1), where both catalyzed and uncatalyzed reactions follow second-order reaction kinetics. However, under the operational conditions (with [**SM1**] ≫ [**SM2**]) we calculate the reaction rate constant based on the pseudo-first order assumption (Equation S1). As is apparent from Figure 1a,c and Table S1, catalyst **C1** (0.4 mM) increases the reaction rate 13-fold with respect to the uncatalyzed reaction. A blank reaction with CB[7] (0.42 mM) alone increases the reaction rate 1.9-fold with respect to the uncatalyzed reaction, indicating that the macrocycle shows a small catalytic activity towards the hydrazone formation reaction.[31] Addition of

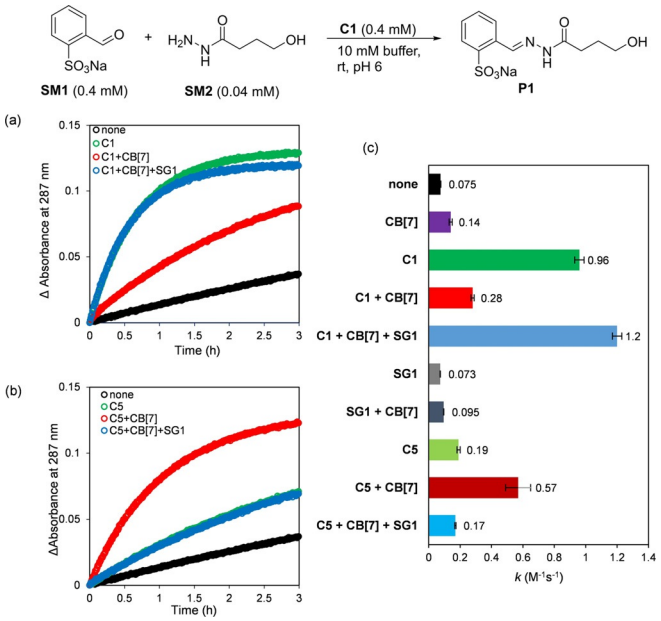

Figure 1. Hydrazone formation catalyzed by **C1** and **C5**: UV-absorbance changes at 287 nm of hydrazone product **P1** followed over time, catalyzed by **C1** (a) and **C5** (b), evaluation of reaction rate constants (c).

CB[7] (0.42 mM) to catalyst **C1** (0.4 mM) should lead to an estimated > 89 % of the catalyst bound in CB[7] [Eq. (S10)]. This mixture gives a reaction rate constant of 0.28 $M^{-1}s^{-1}$, which is 3.5-fold lower than the catalyzed reaction, showing a substantial reduction of the catalytic activity of **C1**. On top of that, hydrazone formation in the presence of CB[7] (0.42 mM), catalyst **C1** (0.4 mM) and signal molecule **SG1** (0.8 mM) gives a reaction rate constant of 1.2 $M^{-1}s^{-1}$, showing that the signal molecule effectively replaces the catalyst by competitive binding with CB[7], restoring the catalytic activity of catalyst **C1**. Noteworthy, the reaction rate in the presence of CB[7], catalyst **C1** and signal molecule **SG1** is slightly higher than the reaction rate with only catalyst **C1**. A reason might be that the catalytic activity of CB[7] adds up to the catalytic activity of catalyst **C1**, leading to a higher reaction rate. Signal guest molecule **SG1** (0.8 mM) alone does not show any catalytic activity, while the reaction in the presence of CB[7] (0.42 mM) and signal guest **SG1** (0.8 mM) is 1.3-fold faster than the blank reaction, showing that a guest inside the cavity of CB[7] does not have a significant effect on the CB[7] catalytic background activity. In essence, CB[7] encapsulation thus reduces the catalytic activity of organocatalyst **C1**, which can be restored by competitive binding with a signal molecule.

Control over DABCO (C2) catalysis in allylic substitution

The successful control of the hydrazone formation reaction rate via CB[7] catalyst encapsulation encouraged us to extend the application of this strategy to other organocatalysts. 1,4-Diazabicyclo[2.2.2]octane (DABCO, **C2**) is a widely used catalyst in many organic reactions.[32] From ITC, we

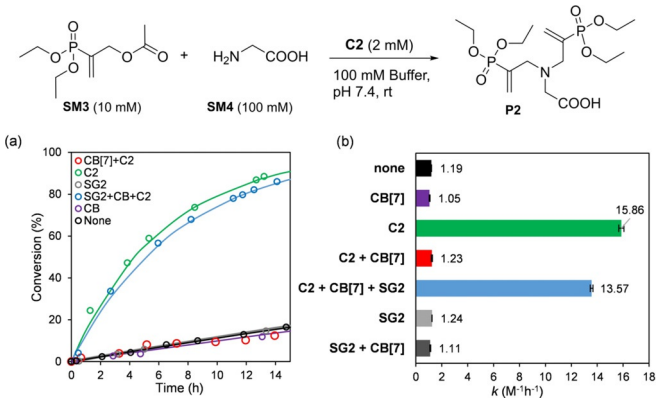

Figure 2. Allylic substitution catalyzed by **C2**: **SM3** conversion followed by ^{1}H NMR (a), evaluation of reaction rate constants (b). Markers indicate experimental data; lines indicate fitted kinetic models.

learned that the binding constant of DABCO (**C2**) with CB[7] is 3.6×10^5 M^{-1} (Table 1), which is in a similar range as **C1** and a suitable value for reaction rate control. Moreover, DABCO was reported to accelerate the allylic substitution reaction between diethyl(α-acetoxymethyl) vinylphosphonate **SM3** and nitrogen-based nucleophiles in aqueous solvents.[33,34] Hence, we used glycine (**SM4**; 100 mM) as nucleophile in phosphate buffer (100 mM, pH 7.4) to react with **SM3** (10 mM), giving the double substituted compound as the major product (Figure 2). Similar to the hydrazone reaction, with **[SM4]** ≫ **[SM3]** in this substitution reaction, we measured a pseudo-first order reaction rate by ^{1}H NMR following the consumption of **SM3** (Figure S2). With 20 mol % of DABCO (2 mM), the **SM3** consumption is 13-fold faster than the uncatalyzed reactions conditions (15.86 $M^{-1}h^{-1}$ vs. 1.19 $M^{-1}h^{-1}$; Figure 2 a,b). Addition of 3.5 mM CB[7], encapsulating about 99.8 % of the present DABCO, decreased the reaction constant to 1.23 $M^{-1}h^{-1}$, giving a similar rate constant as the blank reaction. To avoid any side-reactions of the substrate with **SG1** (a primary amine) signal molecule, **SG2** was used in this particular system to release the catalyst. In the presence of CB[7] (3.5 mM), catalyst **C2** (2 mM, 20 %) and signal molecule **SG2** (6 mM), the reaction rate is accelerated again, about 11.4-times faster than the blank reaction, although slightly lower than the catalytic reaction which may be cause by the slight inhibitory effect of CB[7] itself on this reaction (Figure 2 b). Neither the signal molecule **SG2** (6 mM), or CB[7] (3.5 mM) separately or together show any catalytic activity. This demonstrates a successful reactivation of the substitution reaction through the release of catalyst **C2** from the CB cavity by competitive binding of the signal molecule. From these results, we prove that the catalytic activity of DABCO can be tuned by CB[7] encapsulation and competitive binding of a signal molecule.

Control over prolinol catalysis in aldol reaction

Host-guest regulation of catalytic activity is also applicable to the aldol reaction, one of the most popular synthetic and biochemical means to construct carbon-carbon bonds. The aldol reaction can be catalyzed by a variety of organo-

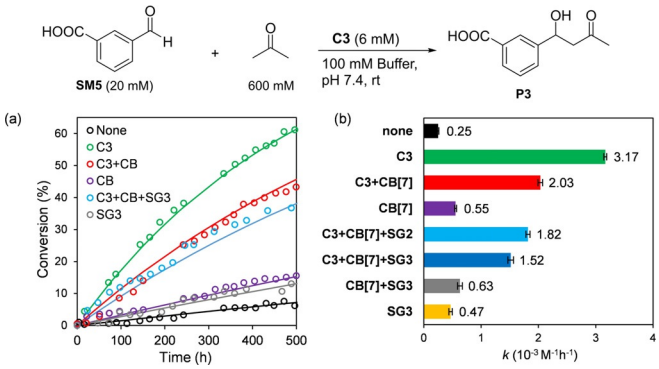

Figure 3. Aldol reaction catalyzed by **C3**: **SM5** conversion followed by ^{1}H NMR (a) and evaluation of reaction rate constants (b). Markers indicate experimental data; lines indicate fitted kinetic models.

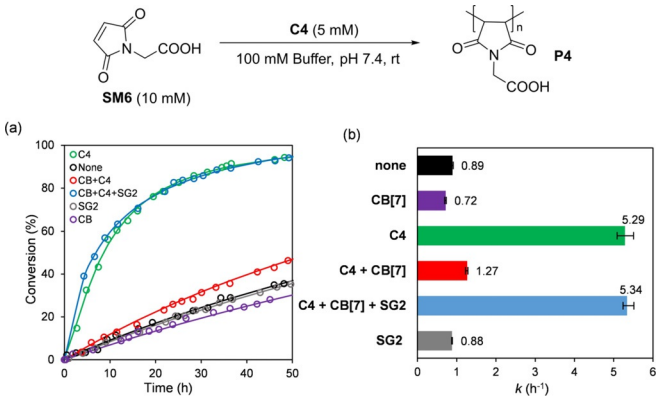

Figure 4. Maleimide oligomerization initiated by **C4**: Conversion of **SM6** followed by ^{1}H NMR (a), evaluation of reaction rate constants (b). Markers indicate experimental data; lines indicate fitted kinetic models.

catalysts in aqueous media.[35–37] We selected a water-soluble aldehyde substrate (**SM5**) as aldol acceptor that with acetone as aldol donor generates aldol product **P3** (Figure 3). This reaction is catalyzed by L-prolinol (**C3**), which has a moderate binding affinity towards CB[7] (Table 1). Without the catalyst, the aldehyde substrate **SM5** (20 mM) with acetone (600 mM, 30 equiv.) in phosphate buffer (100 mM, pH 7.4) shows almost no conversion to **P3** (Figure 3a). However, L-prolinol catalysis (**C3**, 6 mM, 30 mol%) gives a reaction rate constant of 3.17×10^{-3} $M^{-1}h^{-1}$, a 12.7-fold increase relative to the uncatalyzed reaction, under the pseudo-first order conditions ([acetone] ⩾ [**SM5**]). Addition of CB[7] (7 mM) to the catalyzed reaction results in a 36% decrease in the reaction rate. The only moderate rate decrease for this reaction by addition of CB[7] might be caused by the comparably low binding constant of **C3** to CB[7] (5.75×10^3 M^{-1}) and from the unexpectedly high affinity of acetone with CB[7] (592 M^{-1}).[38] In addition, CB[7] itself also has some catalytic activity for this aldol reaction, shown in Figure 3a,b. Remarkably, addition of signal molecules does not result in restoration of catalytic activity of **C3** as would be expected, no matter if the signal molecules are charged (**SG2**) or neutral (**SG3**). The origin of this unexpected result remains unclear, as ^{1}H-NMR did not show unforeseen binding of reaction products or intermediates to CB[7] or the catalyst, which might interfere with catalyst reactivation.

Control over nornicotine in maleimide oligomerization

After demonstrating the capability of CB[7] to control the activity of organocatalysts, we wondered whether the same strategy can be used for the regulation of other organic molecules, such as an organic initiator for polymerization, in order to extend the scope of our strategy. In that context, we used CB[7] to control the oligomerization of a maleimide derivative. Maleimide is a widely used functional building block in polymer materials.[39] The homo-polymerization of maleimide can be initiated through an anionic mechanism by a base initiator, such as an organic pyridine base in aqueous solution.[40,41] As the initiator we used nornicotine **C4**, which has a binding constant of 4.6×10^4 M^{-1} for CB[7] (Figure 4). Moreover, to avoid maleimide *N*-additions as side reactions, *N*-acetic acid maleimide (**SM6**) was synthesized, which also increased substrate solubility and removed any affinity for CB[7]. In the presence of **C4**, the substrate consumption was accelerated (> 90% conversion in 50 h) compared to the initiator-free blank reaction, resulting in a 5.9-fold faster reaction (5.29 h^{-1} vs. 0.89 h^{-1}, Figure 4b). Addition of 7 mM CB[7] into the reaction mixture slowed down the rate to 1.27 h^{-1}. Analogous to the organocatalyzed reactions above, addition of signal molecule **SG2** (12 mM) leads to recovery of the reaction rate back to the same level as with only nornicotine present, while the signal molecule and CB[7] alone did not show any activity.

Catalysis enhancement (C5)

So far, we have demonstrated the inhibiting effect of CB[7] on the activity of organocatalysts **C1**, **C2**, **C3** and initiator **C4**. Yet, CB[7] can also be used to increase organocatalytic activity. 1*H*-benzimidazole-2-methanamine **C5** (0.4 mM) is a catalyst for the same hydrazone formation reaction as shown in Figure 1b,c. Addition of CB[7] (0.42 mM) to that reaction leads to a 3-fold higher reaction rate than the reaction rate with only **C5** (0.57 vs. 0.19 $M^{-1}s^{-1}$). CB[7] encapsulation in this case increased the catalytic activity of **C5**, which is an opposite effect compared to what we observe for catalyst **C1** in the same reaction. Next, addition of signal molecule **SG1** (0.8 mM) to the reaction with catalyst **C5** (0.4 mM) and CB[7] (0.42 mM) gives a reaction rate of 0.17 $M^{-1}s^{-1}$, thus restoring the catalytic activity of catalyst **C5** to its original value. As such, in this opposite activation model the catalyst release from CB[7] with a signal molecule also works effectively. We were interested in exploring the mechanism behind the unexpected inverse effect of CB[7] encapsulation on the two catalysts. ^{1}H-NMR binding studies (Figure S5) indicate that catalyst **C1** is fully sequestered inside the CB[7] host. For catalyst **C5**, ^{1}H-NMR shows that only the aromatic part is inside the host but the aliphatic amine sticks out beyond the CB[7] carbonyl rim

(Figure S9,S10). To further elucidate the mechanism, the pK_a of the two catalysts was measured in the absence and presence of CB[7] by pH dependent UV absorbance experiments (Figure S17).[42] Without CB[7], pK_a values are 4.7 for **C1**, and 3.0 (benzimidazole unit), 7.8 (primary amine unit) for **C5**, which has a good agreement with earlier reports (Table S6).[43,44] Macrocyclic encapsulation is well known to influence the pK_a of the guest molecules inside.[45] In our measurement, the presence of CB[7] increases all the pK_a values of **C1** (4.7 to 6.5) and **C5** (3.0 to 4.8, 7.8 to 8.9, Figure S19,20). Next, we tested **C5** analogs without benzimidazole unit, (1*H*-indol-2-yl)methanamine and benzylamine. Although their pK_a values also increased upon CB[7] binding, these two molecules did not show any catalytic activity enhancement (Figure S21,22). Kool postulates that the proton donating ability of the benzimidazole unit in the transition state of the rate determining step is crucial for catalytic activity. (Scheme S1, **TS1**).[27–29] We now see that CB[7] encapsulation can further enhance the protonation ability of benzimidazole, bringing the pK_a from 3.0 to 4.8 and thus closer to the solvent pH (pH 6.0). Binding to CB[7] increased the pK_a of the benzimidazole ring and thus its protonation equilibrium, enhancing catalytic activity of **C5**.

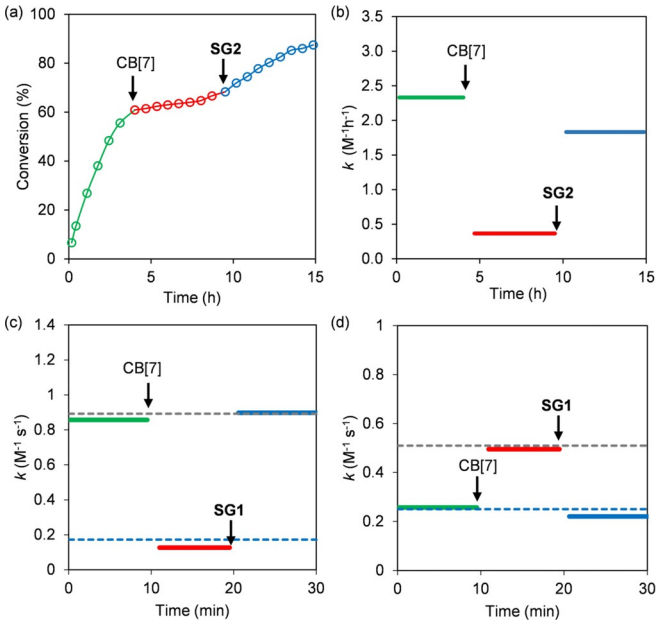

Figure 5. Using CB[7] to control the reaction rate by reversibly binding to the catalyst in situ. a) Conversion of **SM3** in the allylic substitution using **C2**, CB[7] is added after 5 h and **SG2** is added after 10 h; b) Reaction rate constant as a function of time for the allylic substitution depicted in Figure 5 a; c) Reaction rate constant as a function of time for the hydrazone formation reaction using catalyst **C1**, CB[7] is added after 10 min and **SG1** is added after 20 min; d) Reaction rate constant as a function of time for the hydrazone formation reaction using catalyst **C5**, CB[7] is added after 10 min and **SG1** is added after 20 min.

In-situ control over catalytic activity

Using this supramolecular encapsulation strategy, we hypothesized that we should be able to change the reaction rate at any given moment of time during the reaction, by adding CB[7] to encapsulate the catalyst or by releasing the catalyst with addition of a signal molecule. We performed these in situ control experiments with CB[7] for the organocatalysts in the allylic substitution reaction and the hydrazone formation reaction (Figure 5). In the allylic substitution reaction with catalyst **C2** (2 mM), adding CB[7] (3.5 mM) after 5 h caused an immediate flattening of the conversion curve (Figure 5 a), demonstrating that the host molecule can very rapidly change the activity of the catalyst by encapsulating it. Subsequent addition of signal molecule **SG2** after 10 h shifted the curve back to a higher rate. The decrease of the reaction rate constant after CB[7] addition at 5 h and re-initialization with **SG2** at 10 h confirms the effective regulation of the catalytic activity of DABCO (Figure 5 b). Similarly, for catalyst **C1** in the hydrazone formation reaction, we also performed an in situ (de-)activation experiment. When monitoring the reaction using catalyst **C1** (0.4 mM), upon adding CB[7] (0.42 mM) after 10 min we immediately observed a decrease in reaction rate (Figure 5 c). Subsequent addition of signal molecule **SG1** (0.8 mM) after 20 min resulted in an increased reaction rate, back to the original value. For the activated catalyst **C5**, in situ activity control also works. As shown in Figure 5 d, adding CB[7] after 10 min to the reaction mixture with catalyst **C5** (0.4 mM) increases the reaction rate immediately. Addition of signal molecule **SG1** (0.8 mM) 10 min later liberated the catalyst again from the CB[7] cavity restoring the reaction rate to the original level. These results of two reaction examples with three different organocatalysts confirm successful in situ control of the catalytic activity where CB[7] can thus be used to switch off the catalyst, and a signal molecule can switch the system back on again.

A kinetic model to predict reaction rates based on speciation

With this CB[7] responsive catalyst systems in hand, we wondered whether we could control the rate of hydrazone formation precisely by varying the ratio of [catalyst] versus [CB[7]] and predict the reaction rate with a kinetic model. We followed the reactions with different concentrations of catalyst **C1** and CB[7] and determined the reaction rates constants experimentally (Figure 6; black dots). The developed kinetic model to predict the reaction rate constants is shown in Figure 6 (red lines). In the kinetic model we assumed that hydrazone formation occurred without catalyst (k_1), via organocatalysis (k_2), catalyzed by CB[7] (k_3) and catalyzed by the catalyst⊂CB[7] complex (k_4) (Equation 1). The partial reaction rate constants were determined by fitting the concentration profiles of the formation of hydrazone with the least square error method, giving: $k_1 = 0.0568\ M^{-1}s^{-1}$, $k_2 = 2.46 \times 10^3\ M^{-2}s^{-1}$, $k_3 = 150\ M^{-2}s^{-1}$, $k_4 = 221\ M^{-2}s^{-1}$ (see Supplementary information).

$$k_{total} = k_1 + k_2 \cdot [cat] + k_3 \cdot [CB7] + k_4 \cdot [cat \subset CB7] \quad (1)$$

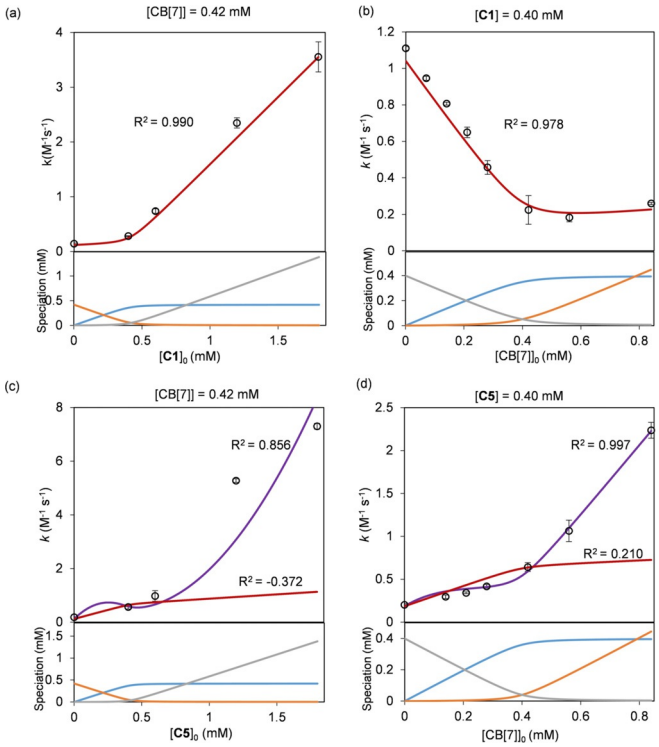

Figure 6. The reaction rate can be controlled precisely by adjusting the ratio of CB[7] and catalyst. The upper graphs show the rate constants for hydrazone formation for varying concentrations of added catalyst and CB[7]. Experimentally determined reaction rate constants are shown as markers and the line represents the kinetic model (see SI). The lower graphs show the varying concentrations of different species in the system depending on the catalyst (**C1** or **C5**) and CB[7] concentration, blue = [Catalyst⊂CB7] (mM), orange = $[CB7]_{free}$ (mM), grey = $[catalyst]_{free}$ (mM). a) The concentration of CB[7] is kept constant at 0.42 mM while the concentration of **C1** is varied between 0–1.8 mM, $R^2 = 0.990$; b) The concentration of **C1** is kept constant at 0.4 mM whereas the concentration of CB[7] is varied between 0–0.84 mM, $R^2 = 0.978$. c) The concentration of CB[7] is kept constant at 0.42 mM whereas the concentration of **C5** is varied between 0–1.8 mM, R^2[Eq. (1)] = −0.372 (red line), R^2[Eq. (3)] = 0.856 (purple line). d) The concentration of **C5** is kept constant at 0.4 mM whereas the concentration of CB[7] is varied between 0–0.84 mM, R^2[Eq. (1)] = 0.210 (red line), R^2[Eq. (3)] = is 0.997 (purple line).

We quantified how well the model (Figure 6, red line) fits the experimental values by determining the coefficients of determination R^2.[46] In Figure 6a we kept the concentration of CB[7] (0.42 mM) constant and varied the concentration of catalyst **C1**. When [**C1**] < [CB[7]], the reaction rate hardly increases due to the inhibiting effect of CB[7] encapsulation, until all CB cavities are occupied and free catalysts become available to the system. When [**C1**] > [CB[7]] the reaction rate increases linearly in the measured concentration range. The highest concentration of catalyst **C1** used was 1.8 mM, where the reaction rate is 25-fold higher than without catalyst **C1**. The reaction rates are predicted well by the linear kinetic model of Equation 1 with an R^2 value of 0.990. In Figure 6b we kept the concentration of catalyst **C1** (0.4 mM) constant and varied the concentration of CB[7]. The reaction rates decreased linearly with increasing CB[7] concentrations until the concentration of CB[7] exceeds the catalyst concentration: then the reaction rate levels off and even increase slightly again, most probably due to the catalytic activity of CB[7] itself (Figure 1). The model predicts the experimental data in Figure 6b with an R^2 value of 0.978. Overall, the kinetic model of Equation (1) predicts the reactions rates well, indicating that the reaction rate constants are a linear combination of all processes taking place, which are in turn proportional to the concentrations (speciation, Figure 6) of all catalytic species involved. This linear relationship allows for precise control over catalytic activity through CB[7] complexation.

In Figure 6c,d we varied the CB[7] to catalyst **C5** ratio. The reaction rates increases dramatically when we keep the concentration of CB[7] (0.42 mM) constant and increase the concentration of catalyst **C5**, up to 39-fold higher with [**C5**] = 1.8 mM than without catalyst (Figure 6c). Similarly, in Figure 6d, the reaction rate also shows a stark increase with increasing excess of CB[7] when the concentration of catalyst **C5** (0.4 mM) is kept constant. These activities are among the highest recorded for hydrazone formation using small molecule catalysts.[27,28,47] The linear kinetic model [Eq. (1)] used before does not describe the measurements (R^2 values of −0.372 and 0.210). When comparing the host-guest-complex speciation (free CB[7], free catalyst **C5**, the **C5**⊂CB[7] complex) at varying ratios of CB[7] and catalyst **C5** to the observed rates, a correlation appears to exist between the rate and the product of the complex and excess species concentrations. Such a correlation suggests the existence of a synergistic effect between the excess species (either free CB[7] or free catalyst **C5**) and the **C5**⊂CB[7] complex that leads to a higher catalytic activity than all species separately. In an attempt to incorporate this synergistic effect into the kinetic model, we extended our existing model with two more extra partial rate constants [Eq. (2)], and adjust this formulation for second-order influence [Eq. (3)]. The new model prediction of the reaction rates in both Figure 6c and d is in much better agreement with the experimental data with R^2 values of, respectively 0.856 and 0.997 (purple line), which suggests that there is indeed a synergistic effect and a second-order influence of catalyst **C5**. Nevertheless, the mechanism behind this synergistic behavior remains unclear, as Equation (2) and (3) indicate that a large number of catalytic species is involved in the rate determining step, which has a reduced likelihood with increasing complexity.

$$k_{total} = k_1 + k_2 \cdot [cat] + k_3 \cdot [CB7] + k_4 \cdot [cat \subset CB7] + k_5 \cdot [CB7] \cdot [cat \subset CB7] + k_6 \cdot [cat] \cdot [cat \subset CB7] \quad (2)$$

$$k_{total} = k_1 + k_2 \cdot [cat] + k_3 \cdot [CB7] + k_4 \cdot [cat \subset CB7] + k_5 \cdot [CB7][cat \subset CB7] + k_6 \cdot [cat]^2 \cdot [cat \subset CB7] \quad (3)$$

Conclusion

In this work, we show that supramolecular encapsulation of organocatalysts with CB[7] is a powerful tool to control and tune catalytic activity. Addition of stoichiometric amounts of CB[7] to the catalysts or initiator leads to an immediate reaction rate decrease for catalysts **C1** to **C4**, where CB[7] acts as an inhibitor, and an rate increase for **C5**, where CB[7]

acts as an activator. Addition of a stronger binding signal molecule restores the reaction rate back to the original value. These events can be carried out in situ, leading to an immediate response. On top of that, we show that adjusting the ratio of catalyst to CB[7] allows precision control over the reaction rate. The experimental data were supported by a kinetic model that accurately predicts the rate of hydrazone formation with catalyst **C1**. For catalyst **C5**, we discovered a disproportionally high increase in reaction rate in non-equimolar mixtures of CB[7] and catalyst **C5**. Fitting this data to a quadratic model suggests a synergistic effect between CB[7], catalyst **C5** and the **C5**⊂CB[7]-complex. Altogether, by using a variety of common, simple, commercially available organocatalysts and different reactions we demonstrated that this strategy is broadly applicable for signal-responsive control of organocatalyst activity. This responsive catalyst system is a step forward in the development of man-made chemical reaction networks and cascades that respond to chemical changes in the environment, as ubiquitously present in nature.

Acknowledgements

Financial support by the Chinese Scholarship Council (G.L.) the Netherlands Organisation for Scientific Research (R.E., NWO Vidi grant) and the European Research Council (R.E., ERC Consolidator Grant 726381) are acknowledged. We thank Dr. P.-L. Hagedoorn and Dr. S. T. Afroza Islam for help with ITC measurements, and Dr. R. Lewis for GPC measurements.

Conflict of interest

The authors declare no conflict of interest.

Keywords: cucurbit[7]uril · host–guest systems · organocatalysis · responsive systems · supramolecular chemistry

[1] G. Ashkenasy, T. M. Hermans, S. Otto, A. F. Taylor, *Chem. Soc. Rev.* **2017**, *46*, 2543 – 2554.
[2] M. P. van der Helm, T. de Beun, R. Eelkema, *Chem. Sci.* **2021**, *12*, 4484 – 4493.
[3] T. W. Traut, *Allosteric Regulatory Enzymes*, Springer, New York, **2008**.
[4] J. Monod, J.-P. Changeux, F. Jacob, *J. Mol. Biol.* **1963**, *6*, 306 – 329.
[5] V. Blanco, D. A. Leigh, V. Marcos, *Chem. Soc. Rev.* **2015**, *44*, 5341 – 5370.
[6] H. J. Yoon, J. Kuwabara, J.-H. Kim, C. A. Mirkin, *Science* **2010**, *330*, 66 – 69.
[7] V. Blanco, A. Carlone, K. D. Hänni, D. A. Leigh, B. Lewandowski, *Angew. Chem. Int. Ed.* **2012**, *51*, 5166 – 5169; *Angew. Chem.* **2012**, *124*, 5256 – 5259.
[8] V. Blanco, D. A. Leigh, V. Marcos, J. A. Morales-Serna, A. L. Nussbaumer, *J. Am. Chem. Soc.* **2014**, *136*, 4905 – 4908.
[9] V. Blanco, D. A. Leigh, U. Lewandowska, B. Lewandowski, V. Marcos, *J. Am. Chem. Soc.* **2014**, *136*, 15775 – 15780.
[10] A. C. H. Jans, A. Gómez-Suárez, S. P. Nolan, J. N. H. Reek, *Chem. Eur. J.* **2016**, *22*, 14836 – 14839.
[11] A. Cavarzan, A. Scarso, P. Sgarbossa, G. Strukul, J. N. H. Reek, *J. Am. Chem. Soc.* **2011**, *133*, 2848 – 2851.
[12] G. Bianchini, A. Scarso, G. La Sorella, G. Strukul, *Chem. Commun.* **2012**, *48*, 12082 – 12084.
[13] J. Czescik, Y. Lyu, S. Neuberg, P. Scrimin, F. Mancin, *J. Am. Chem. Soc.* **2020**, *142*, 6837 – 6841.
[14] G. Y. Tonga, Y. Jeong, B. Duncan, T. Mizuhara, R. Mout, R. Das, S. T. Kim, Y. C. Yeh, B. Yan, S. Hou, V. M. Rotello, *Nat. Chem.* **2015**, *7*, 597 – 603.
[15] D. Song, B. Li, X. Li, X. Sun, J. Li, C. Li, T. Xu, Y. Zhu, F. Li, N. Wang, *ChemSusChem* **2020**, *13*, 394 – 399.
[16] B. Tang, J. Zhao, Y. Jiao, J.-F. Xu, X. Zhang, *Chem. Commun.* **2019**, *55*, 14127 – 14130.
[17] T. G. Brevé, M. Filius, C. Araman, M. P. van der Helm, P. L. Hagedoorn, C. Joo, S. I. van Kasteren, R. Eelkema, *Angew. Chem. Int. Ed.* **2020**, *59*, 9340 – 9344; *Angew. Chem.* **2020**, *132*, 9426 – 9430.
[18] X. Zhang, B. Tang, J. Zhao, J.-F. Xu, *Chem. Eur. J.* **2020**, *26*, 15446 – 15460.
[19] S. Liu, C. Ruspic, P. Mukhopadhyay, S. Chakrabarti, P. Y. Zavalij, L. Isaacs, *J. Am. Chem. Soc.* **2005**, *127*, 15959 – 15967.
[20] L. Isaacs, *Chem. Commun.* **2009**, 619 – 629.
[21] S. J. Barrow, S. Kasera, M. J. Rowland, J. Del Barrio, O. A. Scherman, *Chem. Rev.* **2015**, *115*, 12320 – 12406.
[22] D. W. C. MacMillan, *Nature* **2008**, *455*, 304 – 308.
[23] M. P. van der Helm, B. Klemm, R. Eelkema, *Nat. Rev. Chem.* **2019**, *3*, 491 – 508.
[24] S. Sinn, F. Biedermann, *Isr. J. Chem.* **2018**, *58*, 357 – 412.
[25] A. D. St-Jacques, I. W. Wyman, D. H. Macartney, *Chem. Commun.* **2008**, 4936 – 4938.
[26] S. Moghaddam, C. Yang, M. Rekharsky, Y. H. Ko, K. Kim, Y. Inoue, M. K. Gilson, *J. Am. Chem. Soc.* **2011**, *133*, 3570 – 3581.
[27] P. Crisalli, E. T. Kool, *J. Org. Chem.* **2013**, *78*, 1184 – 1189.
[28] D. Larsen, M. Pittelkow, S. Karmakar, E. T. Kool, *Org. Lett.* **2015**, *17*, 274 – 277.
[29] D. K. Kölmel, E. T. Kool, *Chem. Rev.* **2017**, *117*, 10358 – 10376.
[30] F. Trausel, B. Fan, S. A. P. van Rossum, J. H. van Esch, R. Eelkema, *Adv. Synth. Catal.* **2018**, *360*, 2571 – 2576.
[31] A. Palma, M. Artelsmair, G. Wu, X. Lu, S. J. Barrow, N. Uddin, E. Rosta, E. Masson, O. A. Scherman, *Angew. Chem. Int. Ed.* **2017**, *56*, 15688 – 15692; *Angew. Chem.* **2017**, *129*, 15894 – 15898.
[32] A. Abdel-Aziem, M. S. El-Gendy, A. O. Abdelhamid, *Eur. J. Chem.* **2012**, *3*, 455 – 460.
[33] C. Garzon, M. Attolini, M. Maffei, *Tetrahedron Lett.* **2010**, *51*, 3772 – 3774.
[34] A. Seingeot, Y. Charmasson, M. Attolini, M. Maffei, *Heteroat. Chem.* **2017**, *28*, e21352.
[35] T. J. Dickerson, K. D. Janda, *J. Am. Chem. Soc.* **2002**, *124*, 3220 – 3221.
[36] N. Mase, Y. Nakai, N. Ohara, H. Yoda, K. Takabe, F. Tanaka, C. F. Barbas, *J. Am. Chem. Soc.* **2006**, *128*, 734 – 735.
[37] M. Raj, V. K. Singh, *Chem. Commun.* **2009**, 6687 – 6703.
[38] I. W. Wyman, D. H. Macartney, *Org. Biomol. Chem.* **2008**, *6*, 1796 – 1801.
[39] E. Dolci, V. Froidevaux, C. Joly-Duhamel, R. Auvergne, B. Boutevin, S. Caillol, *Polym. Rev.* **2016**, *56*, 512 – 556.
[40] D. Decker, *Makromol. Chem.* **1973**, *168*, 51 – 58.
[41] M. Azechi, N. Toyota, K. Yamabuki, K. Onimura, T. Oishi, *Polym. Bull.* **2011**, *67*, 631 – 640.
[42] N. Barooah, M. Sundararajan, J. Mohanty, A. C. Bhasikuttan, *J. Phys. Chem. B* **2014**, *118*, 7136 – 7146.
[43] E. H. Cordes, W. P. Jencks, *J. Am. Chem. Soc.* **1962**, *84*, 826 – 831.
[44] A. Sierra-Zenteno, C. Galán-Vidal, R. Tapia-Benavides, *Rev. Soc. Quim. Mex.* **2002**, *46*, 125 – 130.

[45] I. Ghosh, W. M. Nau, *Adv. Drug Delivery Rev.* **2012**, *64*, 764 – 783.
[46] L. Magee, *Am. Stat.* **1990**, *44*, 250 – 253.
[47] Y. Zhou, I. Piergentili, J. Hong, M. P. van der Helm, M. Macchione, Y. Li, R. Eelkema, S. Luo, *Org. Lett.* **2020**, *22*, 6035 – 6040.

Manuscript received: February 12, 2021
Revised manuscript received: March 24, 2021
Accepted manuscript online: April 5, 2021
Version of record online: May 7, 2021

